

# **X-34 MAIN PROPULSION SYSTEM - SELECTED SUBSYSTEM ANALYSES**

T. M. Brown, J. P. McDonald, K. C. Knight  
Propulsion Department, Sverdrup Technology Inc.  
Marshall Space Flight Center Group  
Huntsville, Alabama

1N-20  
432218

R. H. Champion, Jr.  
Marshall Space Flight Center  
Huntsville, Alabama

## **Abstract**

The X-34 hypersonic flight vehicle is currently under development by Orbital Sciences Corporation (Orbital). The Main Propulsion System (MPS) has been designed around the liquid propellant Fastrac rocket engine currently under development at NASA Marshall Space Flight Center. This paper presents selected analyses of MPS subsystems and components. Topics include the integration of component and system level modeling of the LOX dump subsystem and a simple terminal bubble velocity analysis conducted to guide propellant feed line design.

## **Introduction**

The X-34 vehicle is to be capable of hypersonic flight (Mach 8) at altitudes of 250,000 feet. The X-34 vehicle Main Propulsion System (MPS) utilizes the Liquid Oxygen (LOX) and kerosene (RP-1) Fastrac rocket engine<sup>1</sup> currently under development at NASA Marshall Space Flight Center (MSFC). Detailed overviews of the entire X-34 propulsion system have been provided by Sgarlata and Winters<sup>2</sup> and Sullivan and Winters.<sup>3</sup> The X-34 vehicle will be launched from the bottom of an L1011 aircraft after being carried to an altitude of 38,000 feet. The horizontal flight of the X-34 vehicle, coupled with many aggressive operational goals, have created several challenges not normally considered in conventional vertical flight rockets.

Detailed analyses of the MPS subsystems were required initially as design inputs, and later for design validation and verification. Analysis of X-34 MPS propellant management and conditioning has been presented previously by Brown et al.<sup>4</sup> Propellant feed and pressurization systems have been covered in detail by McDonald et al.,<sup>5</sup> and Hedayat et al.,<sup>6</sup> respectively. This paper presents only selected analyses of MPS subsystems and components. The first section covers analysis of the LOX dump subsystem, including the integration of detailed component level analysis in system level modeling. The second section presents a simple bubble buoyancy/terminal velocity analysis, conducted to guide the design of the propellant feed system.

The general layout of much of the X-34 MPS within the X-34 vehicle is presented in Figure 1. Figure 2 is an abbreviated MPS schematic. LOX is stored in two compartmentalized tanks. The LOX dump/feed/drain system is connected to the aft end of the rear LOX tank and includes an exit orifice to maintain static pressure within the system above the saturation point. The LOX feed system is also connected to the aft end of the rear LOX tank. The high point of the LOX feed system is the tank/feed line interface. RP-1 is stored in a single compartmentalized tank.

The RP-1 system has a common feed, dump, drain and fill line for much of the vehicle length, with separate lines and valves at the tank and the aft end. The aft portion of the RP-1 feed line has a vertical section just in front of the engine thrust structure. The line then loops over the thrust structure and down to the engine inlet. This high point in the RP-1 feed line requires careful consideration because it may trap gasses during turbopump chill procedures. Trapped gasses could be ingested during engine burn, leading to pump cavitation and a catastrophic failure.

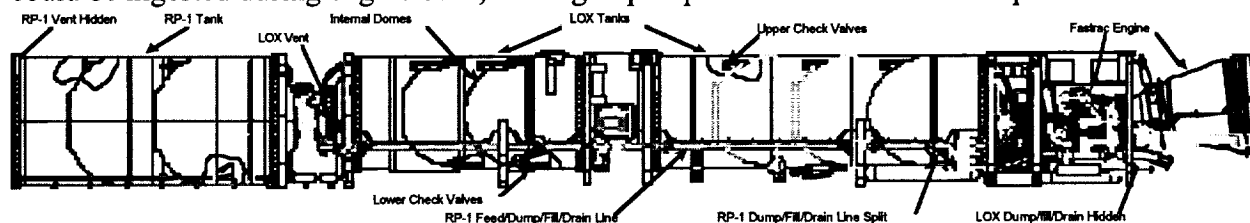


Figure 1. MPS Layout Within the X-34 Vehicle.

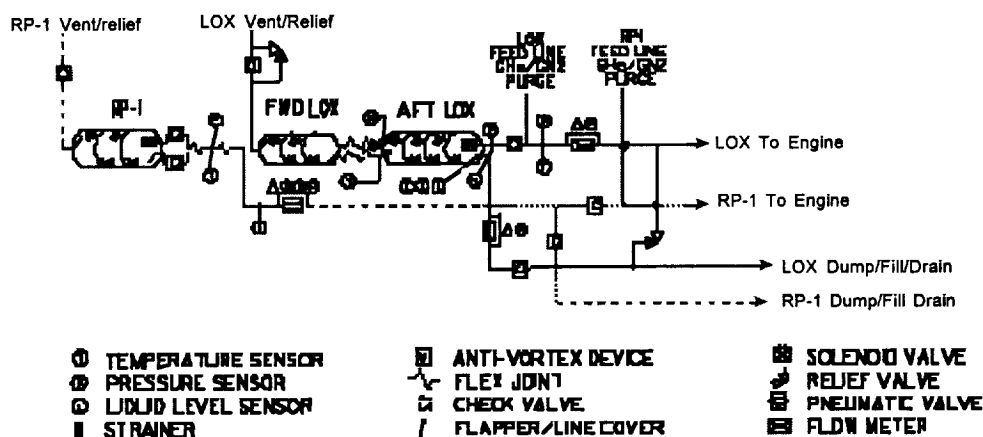


Figure 2. Schematic of the Propellant Management Subsystems.

### LOX Dump System Analysis

The LOX and RP-1 dump systems have both been modeled using the Generalized Fluid System Simulation Program (GFSSP).<sup>7</sup> LOX system analysis was slightly more complicated because it required modeling critical fluid flow through an exit orifice. The exit orifice is required to maintain local static pressures, within the LOX dump system, above the saturation pressure of the LOX to be dumped, thus preventing vaporization. Vaporization is undesirable since large density changes cause locally high flow velocities, thus increasing particle impact ignition concerns. Also, vaporization within the LOX dump flow meter results in improper propellant gauging by the flight computer.

The X-34 abort design reference mission results in a 3 psia dump system exit pressure. Lower exit pressures may occur during a robust abort scenario. The exit orifice pressure drop must be large enough to maintain the static pressure within the dump line above 13 psia. For a 3.0 inch diameter orifice within a 3.384 inch ID dump line and 0.79 flow coefficient, GFSSP predicts the pressure drop and mass flow rate to be 16 psi and 146 lbm/sec, respectively. This

flow coefficient corresponds to a completely immersed orifice, but here, a LOX free shear jet in air exists downstream of the orifice. Thus, a CFD simulation of the dump exit was performed to better define the orifice flow coefficient.

#### CFD Simulation of Orifice Performance

A constant mass flow rate boundary condition of 146 lbm/sec is used to determine the static pressure profile across the orifice. Figure 3 illustrates the steady-state centerline pressure profile from a Flow3D<sup>8</sup> simulation of the exit orifice. The pressure profile in Figure 3 indicates a static pressure drop of 11.5 psi across the orifice for the 146 lbm/sec. flow rate.

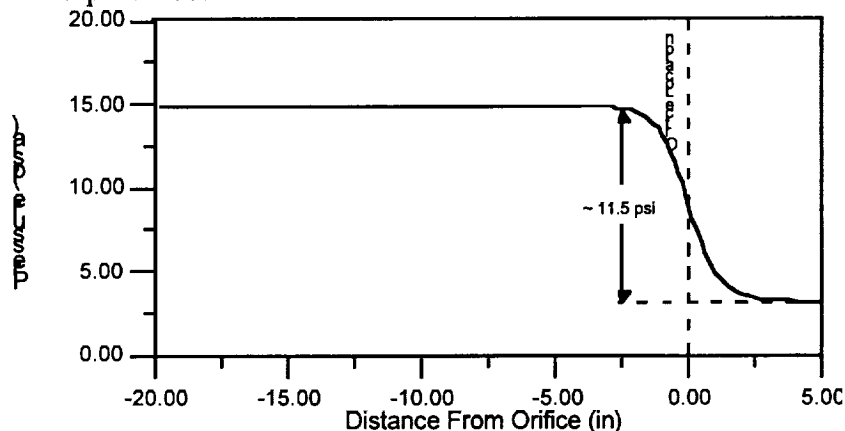


Figure 3. Centerline Pressure Profile of the LOX Dump System Exit.

#### Orifice Flow Coefficient Determination

A better estimation of the orifice flow coefficient was obtained by coupling the CFD results with a GFSSP model. With pressure boundary conditions and fluid properties identical to those from the CFD simulation, the orifice flow coefficient was adjusted in the GFSSP model to match the mass flow rate of 146 lbm/sec. The resultant orifice flow coefficient of 1.1 was used in subsequent system level GFSSP simulations.

#### LOX Dump System Performance Simulation

GFSSP simulations of the entire dump system were run using the CFD derived orifice flow coefficient. Table 1 lists the results for various operating conditions.

<u>Tank Pressure (psia)</u>	<u>Exit Pressure (psia)</u>	<u>Mass Flow (lbm/sec)</u>	<u>Orifice ΔP (psi)</u>
58	15	140	10.5
58	10	147	11.8
58	6	154	12.7
58	3	158	13.5
58	0.5	161	14.1

Table 1. LOX Dump System Performance Simulation Results

The minimum static pressure within the dump system is the exit pressure plus the orifice pressure drop. The results presented in Table 1 indicate that even at very low exit pressures, the original 3 inch orifice maintains the static pressure within the dump system above 14 psia.

Under normal (DRM3) dump procedures, the minimum dump exit pressure will be  $\sim 3$  psia. Table 1 indicates that, under these conditions, the minimum static pressure within the dump system will be 16.5 psia. This pressure precludes vaporization for the highest anticipated LOX condition temperatures. While substantial deviations from the line/orifice size modeled by Flow3D require new estimates of the flow coefficient, the 1.1 value above is otherwise sufficient for use in GFSSP system level analyses.

### RP-1 Feed Line High Point Bleed Consideration

A high point exists in the RP-1 feed line where it avoids the engine thrust structure at the aft end of the X-34 vehicle. This high point in the RP-1 feed line requires careful consideration because it may trap gasses during turbopump chill procedures. Trapped gasses could be ingested during engine burn, leading to pump cavitation and a catastrophic failure. This analysis is intended to determine the minimum RP-1 velocity required to purge the trapped gas from the high point in the feed line. A high point bleed is required if sufficient flow velocities are not reached during turbopump chill procedures.

Figure 3 depicts a static gas bubble in a liquid flow field. The bubble will remain static if the buoyancy force is equal to the drag force ( $\Sigma F_y = F_b - F_d = 0$ ).

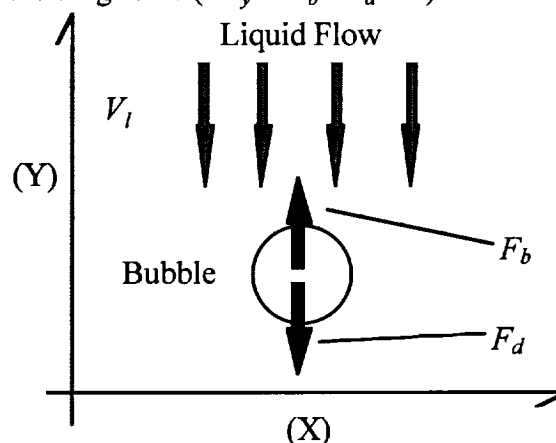


Figure 3. Static Gas Bubble in a Liquid Flow Field

The coefficient of drag for a sphere is described by the following equation,<sup>9</sup>

$$Cd = \frac{F_d}{\frac{1}{2} \rho_l V_l^2 \frac{\pi}{4} d^2}$$

where  $F_d$  is the drag force,  $\rho_l$  is the liquid density,  $V_l$  is the liquid velocity and  $d$  is the bubble diameter. Therefore, the drag force on the sphere is,

$$F_d = Cd \frac{1}{2} \rho_l V_l^2 \frac{\pi}{4} d^2.$$

The buoyancy force is given by,

$$F_b = Vol_b \rho_l g - Vol_b \rho_b g \quad \text{or} \quad F_b = \frac{\pi}{6} d^3 g (\rho_l - \rho_b)$$

The drag force ( $F_d$ ) must be equal to the buoyancy force ( $F_b$ ) for the bubble to remain static. Therefore,

$$F_d = F_b \quad \text{and,} \quad V_l = \sqrt{\frac{4}{3} \frac{d}{Cd} g \frac{(\rho_l - \rho_b)}{\rho_l}}.$$

This equation gives the velocity that will create a drag force offsetting the buoyancy of the bubble. Liquid velocities greater than  $V_l$  will carry the bubble along with the flow, while velocities lower than  $V_l$  will allow the bubble to rise.

In the case of interest, the liquid is RP-1 and the bubble contains nitrogen. Because the density of nitrogen is much less than the density of RP-1, the equation for  $V_l$  simplifies to,

$$V_l = \sqrt{\frac{4}{3} \frac{d}{Cd} g}.$$

Figure 4 presents a plot of  $V_l$  as a function of bubble diameter. In this case  $Cd$  is assumed to be 0.5.

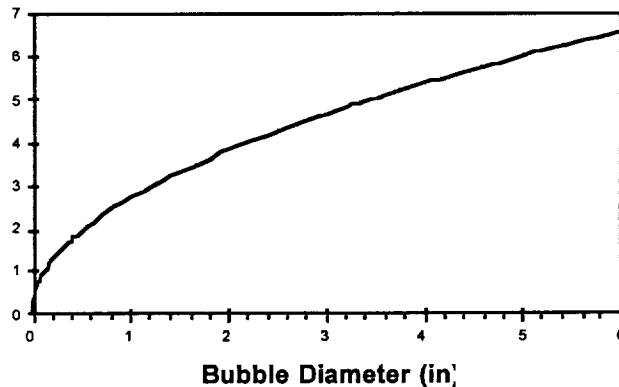


Figure 4. Liquid Velocity Required to Offset the Buoyancy of a Bubble.

The X-34 RP-1 feed line has a diameter of 3.5 in. Therefore, the largest possible bubble diameter is 3.5 in. Figure 4 indicates that the RP-1 velocity must be greater than 5 ft/s to purge the gas bubble from the feed line. The RP-1 flow rate during turbopump chill is  $\sim 2$  lbm/s which corresponds to a flow velocity of  $\sim 0.6$  ft/s. This velocity is much too low to purge the gas from the feed line prior to engine start. Therefore, a high point bleed is required to remove the gas prior to turbopump chill procedures.

### References

1. Fisher, M., and Ise, M., (1998) "Low Cost Propulsion Technology at the Marshall Space Flight Center - Fastrac Engine and the Propulsion Test Article," AIAA Paper No. AIAA-98-3365.
2. Sgarlata, P., and Winters, B., (1997) "X-34 Propulsion System Design," AIAA Paper No. AIAA-97-3304.

3. Sullivan, B. and Winters, B. (1998) "X-34 Propulsion System Overview," AIAA Paper No. AIAA-98-3516.
4. Brown, T. M., McDonald, J. P., Hedayat, A., Knight, K. C., and Champion, R. H. Jr., (1998) "Propellant Management and Conditioning Within the X-34 Main Propulsion System," AIAA Paper No. AIAA-98-3518.
5. McDonald, J. P., Minor, R. B., Knight, K. C., Champion, R. H. Jr., and Russell, F. J. Jr., (1998) "Propellant Feed Subsystem for the X-34 Main Propulsion System," AIAA Paper No. AIAA-98-3517.
6. Hedayat, A., Steadman, T. E., Brown, T. M., Knight, K. C., White, C. E., and Champion, R. H. Jr., (1998) "Pressurization, Pneumatics, And Vent Subsystems of the X-34 Main Propulsion System," AIAA Paper No. AIAA-98-3519.
7. Majumdar, A. K., Bailey, J. W., Schallhorn, P. A., and Steadman, T., (1998) "A Generalized Fluid System Simulation Program to Model Flow Distribution in Fluid Networks," AIAA Paper No. AIAA-98-3682.
8. FLOW-3D Version 6.0, Flow Science, Inc., Los Alamos, NM
9. White, F. M., (1979) "Fluid Mechanics" McGraw-Hill, Inc.